

MULTI CRITERION PRIORITY ON KRIGING OF GOLD RESOURCES PREDICTION

Nur Ali Amri, Waterman Sulistyana Bargawa, Tedy Agung Cahyadi
Universitas Pembangunan Nasional Veteran Yogyakarta
Corresponding author: nuraliamri@upnyk.ac.id

ABSTRACT

This paper describes of three things. First, the Kriging estimation on gold grade which is distributed in the vein. The empirical variogram method based on Matheron classical and robust of Cressie-Hawkins. The two empirical fitting on variogram theory of spherical and exponential equations of weighted least squares and ordinary least squares used. The predictions of six sizes block-Kriging respectively, 15×15, 25×25, 35×35, 50×50, 75×75 and 100×100 based on four variographic models. Second, determine the priority of 24 prediction combinations based on TOPSIS method. Finally, the multiple criterion decision making method namely, 15×15 block Kriging based on a robust empirical variogram of exponential weighted least squares model represents as the best result.

Keywords: Variogram, fitting, block Kriging, TOPSIS.

INTRODUCTION

Gold ores in the vein are formed through the process of mineralization and are strongly influenced by hydrothermal processes [1, 2]. In geology, a vein is a distinct sheet like body of crystallized minerals within a rock. Veins form when minerals constituents carried by an aqueous solution within the rock mass are deposited through precipitation [3]. The hydraulic flow is involved due to hydrothermal circulation [4]. Veins are of prime importance for minerals deposits, because they are the source of mineralization either in or proximal to the veins. Ores is related to hydrothermal mineralization [5], which is associated with vein material, may be composed of vein material and / or the rock in which the vein is hosted [6]. Physically the vein of the study area is elongated, hundreds to thousands of meters long, with a thickness of several hundred meters [7].

The importance of this study is to estimate the distribution of gold deposits in ore veins and values of grade averages and error variances. The results of the kriging estimation based on various models resulting from variogram fittings, where the choice of the best alternative uses multi criteria determination. Because the distribution of gold content is part of the spatial process [8-11], the grade estimation

process uses the geostatistics method. Kriging is a technique in geostatistics that is widely used in spatial cases [12-17], especially in the mining industry [18-20].

MATERIALS AND METHODS

Location

The research location is a mountainous area in the Pongkor gold ore field. Administratively, it is located in the Bayah sub-district, Lebak district, Banten province Indonesia with an elevation of 1,110-1,250m above sea level. Pongkor mineralization has a veins system with the main sub-parallel, quartz-calcite. Vein in this area extends around 700 to 2,500m. Vein thickness is several meters and a depth of more than 200m in the direction of the Northwest-Southeast. Most of this area is widespread weathering which results in gold ore mineralization. The data of this study are the results of assaying 128 random samples derived from core drilling in the Ciurug vein with an area of about 1,500×370m².

Variogram

The occurrence of gold ore, which is distributed in the vein model, allows the occurrence of spatial properties, namely the nature of correlating between data in an area. Therefore, tracing of this behavior is constructed through a variogram model approach [21]. Two empirical variograms [22, 23] using the term variance used in this approach are the Matheron's variogram [24] and Cressie-Hawkins model known as the robust method [10, 11]. Empirical variogram is a formula used to determine spatial correlation between data in an area. Mathematically presents as follows:

$$\hat{\gamma}(\mathbf{h}) = \frac{1}{2|N(\mathbf{h})|} \sum_{N(\mathbf{h})} (Z(\mathbf{s}_i) - Z(\mathbf{s}_j))^2; \mathbf{h} \in \mathbb{R}^d. \quad (1)$$

While the robust method is presented as,

$$\bar{\gamma}(\mathbf{h}) = \frac{\left(\frac{1}{2|N(\mathbf{h})|} \sum_{N(\mathbf{h})} (Z(\mathbf{s}_i) - Z(\mathbf{s}_j))^{1/2} \right)^4}{\left(0.457 + \frac{0.494}{|N(\mathbf{h})|} \right)}; \mathbf{h} \in \mathbb{R}^d \quad (2)$$

$N(\mathbf{h}) = \{(\mathbf{s}_i, \mathbf{s}_j) : \|\mathbf{s}_i - \mathbf{s}_j\| = \mathbf{h}; i, j = 1, \dots, n\}$ dan $|N(\mathbf{h})|$ is the number of pairs of points with lag \mathbf{h} .

Fitting

Practically the formulas (1) and (2) are empirical equations that produce discrete points. To obtain good graphics, refining with fittings is very necessary. The two fitting processes used in this paper are ordinary least squares (OLS) and weighted least squares (WLS) methods [25, 26]. The theoretical formula of variogram used to obtain variogram parameters is spherical and exponential models, as shown in Table 1. Co is the nugget value, Co + C is sill, while the range is denoted as α . Spherical

models are mathematical formulas for fitting processes that are often used in the mining industry [27, 28], while the exponential model is a comparison.

Ordinary Kriging

One of several gold grade estimation techniques is ordinary kriging [29] as the best linear unbiased predictor (BLUP). OK method is a data interpolation technique, by estimating the spatial value around the data [30]. This technique uses the stationary concept, which is considered as a stochastic process because it tries to select the weights optimally by minimizing estimation error variance [10, 11].

Suppose there are n sample data $z(\mathbf{s}_i)$ located at several locations \mathbf{s}_i (the value $\mathbf{s}_i \in \mathbb{R}^d$, d in this case having dimension of 2, $i=1, \dots, n$) and \mathbf{s}_0 are the position of the points to be estimated, then the estimation value, $\hat{Z}(\mathbf{s}_0)$ can be written as [11]:

$$\hat{Z}(\mathbf{s}_0) = \sum_{i=1}^n w_i z(\mathbf{s}_i). \quad (3)$$

where the sum of the total weights w_i is one.

Based on $\tilde{\boldsymbol{\gamma}} = \sum_{i=1}^n (\mathbf{s}_0 - \mathbf{s}_i)$ and $\Gamma = \sum_{i=1}^n \sum_{j=1}^n \gamma(\mathbf{s}_i - \mathbf{s}_j)$, in matrix the weight $\tilde{\mathbf{w}}$ can be obtained. The weight matrix is:

$$\tilde{\mathbf{w}} = \Gamma^{-1} \tilde{\boldsymbol{\gamma}} \quad (4)$$

The estimation results are used to determine the distribution of values in the mining application to meet the cut-off grade [31]. While error variance is defined by [11, 32, 33]. The gold ore grade estimation uses the geoR library of R package and several other libraries [34].

TOPSIS

Techniques for order preference by similarity to ideal solution (TOPSIS) is a multicriteria decision-making techniques [35-39]. In 1981 Yoon and Kim introduced the TOPSIS method [40]. The main principle of this method is to choose the points with the shortest distance as positive ideal solutions and the farthest distance as the ideal negative solution. Several stages in the completion of this method have been carried out by [41]. These stages are:

1. Preparation of a ranking matrix ($m \times n$), whose elements are the values of scoring. Elements X_{ij} is a measure of alternative choices, i and j -criteria in the matrix and use the following formula:

$$D = \sum_{i=1}^m X_{ij}; j=1, \dots, n. \quad (5)$$

2. Make a normalized decision matrix, where the elements i.e., r_{ij} are derived from:

$$r_{ij} = \frac{X_{ij}}{\sqrt{\sum_{i=1}^m X_{ij}^2}}; j=1, \dots, n. \quad (6)$$

3. Normalized weight matrix elements (V_{ij}) are arranged based on the results of the normalized decision matrix multiplication with the weight matrix, as follows:

$$V_{ij} = \sum_{i=1}^m w_i r_{ij}; j=1, \dots, n. \quad (7)$$

4. Determining the value of positive ideal solutions and negative ideal solutions. The ideal solution is denoted as A^+ , when the negative ideal solution is denoted as A^- . The equation for determining the ideal solution using formula:

$$\begin{aligned} A^+ &= \{(\max V_{ij} | j \in J), (\min V_{ij} | j \in J')\} = \{v_1^+, v_2^+, \dots, v_m^+\} \\ A^- &= \{(\max V_{ij} | j \in J'), (\min V_{ij} | j \in J)\} = \{v_1^-, v_2^-, \dots, v_m^-\} \\ J &= \{j=1, \dots, n\} \text{ associated with benefit criteria} \\ J' &= \{j=1, \dots, n\} \text{ associated with cost criteria.} \end{aligned} \quad (8)$$

5. Calculate separation measure. Separation measure is a measurement of distance from an alternative to a positive ideal solution and a negative ideal solution. Calculation of positive ideal solutions is:

$$S_i^+ = \sqrt{\sum_{j=1}^n (V_{ij} - v_j^+)^2}; j=1, \dots, m. \quad (9)$$

While the calculation of negative ideal solutions is:

$$S_i^- = \sqrt{\sum_{j=1}^n (V_{ij} - v_j^-)^2}; j=1, \dots, m \quad (10)$$

6. Calculate preference values for each alternative. Value of preference calculation for each alternative is carried out to determine the ranking of each alternative. Calculation of this preference value is:

$$\begin{aligned} C_i^+ &= \frac{S_i^-}{S_i^- + S_i^+}; \quad 0 < C_i^+ < 1 \text{ and } i=1, \dots, m \\ C_i^- &= \frac{S_i^+}{S_i^- + S_i^+}; \quad 0 < C_i^- < 1 \text{ and } i=1, \dots, m \end{aligned} \quad (11)$$

Alternative values are ranked according to sequence. From the results of the ranking, it can be concluded that the best alternative is the one that has the shortest distance from the position of the positive ideal solution and the furthest from the negative ideal solution.

RESULT AND DISCUSSION

Geostatistics

This method begins by making an empirical variogram construction as in formula (1) and (2), by first determining the lag distance sequentially, starting from the first lag where, $h = 17.5m$. The maximum lag distance is 500m, and this is the maximum one-third span (x -axis) of the study area. Both distances are simulation products

that are closest to the basic characteristics of variogram. Both empirical variograms (classical and robust) and error values (root mean square error, RMSE) are based on the exponential theoretical approaches of the WLS and OLS models shown by TABLE 1.

The first column presents lag distance, the second and third columns are a collection of values resulting from classical variogram calculations ($\hat{\gamma}(\mathbf{h})$) and robust ($\bar{\gamma}(\mathbf{h})$). The last four columns show error values based on each fitting model. Notation C on CWLSE (Classical Weighted Least Squares Exponential) refers to a classical variogram. The letter E at the last denotation describes a theoretical variogram, which is an exponential function.

TABLE 1 Classical and robust variogram with RMSE value

Lag	RMSE			
	CWLSE	COLSE	RWLSE	ROLSE
1	0.754	1.032	0.700	0.453
2	0.547	0.137	0.838	0.453
3	1.846	2.299	2.424	2.875
4	1.165	0.719	0.591	0.122
5	0.466	0.876	0.244	0.701
6	1.079	0.717	0.174	0.254
7	0.440	0.129	0.831	0.442
8	0.555	0.815	1.470	1.817
9	0.318	0.533	0.144	0.162
10	1.672	1.012	1.573	1.308
11	0.176	0.187	0.314	0.542
12	1.084	1.073	0.509	0.175
13	0.229	0.240	1.013	1.007
14	0.453	0.464	0.438	0.432
15	0.137	0.126	0.066	0.060
16	0.308	0.297	0.921	0.927
17	0.227	0.216	0.362	0.368
18	0.337	0.348	1.004	0.998
19	1.061	1.072	1.542	1.536
20	1.854	1.865	2.591	2.585
21	0.803	0.814	1.454	1.448
22	0.847	0.836	0.487	0.493
23	0.898	0.887	0.817	0.823
24	0.081	0.070	0.693	0.699
25	1.581	1.592	0.594	0.588
26	2.134	2.123	1.147	1.153
27	4.442	4.431	3.585	3.591
28	5.987	5.976	7.012	7.018
Mean	1.124	1.103	1.198	1.179

TABLE 2. List of variogram models as mathematics formula

Fitting base	Practical exponential variogram
CWLSE	$\begin{cases} 11.743 \left[1 - \exp\left(-\frac{ h }{173.169}\right) \right]; & 0 \leq h \leq 173.169 \\ 11.743; & h > 173.169 \end{cases}$
COLSE	$\begin{cases} 11.754 \left[1 - \exp\left(-\frac{ h }{192.706}\right) \right]; & 0 \leq h \leq 192.706 \\ 11.754; & h > 192.706 \end{cases}$
RWLSE	$\begin{cases} 11.611 \left[1 - \exp\left(-\frac{ h }{209.176}\right) \right]; & 0 \leq h \leq 209.176 \\ 11.611; & h > 209.176 \end{cases}$
ROLSE	$\begin{cases} 11.605 \left[1 - \exp\left(-\frac{ h }{233.228}\right) \right]; & 0 \leq h \leq 233.228 \\ 11.605; & h > 233.228 \end{cases}$

The letter R on ROLSE (Robust Ordinary Least Squares Exponential) states that fittings are based on robust empirical variogram with ordinary least squares model. The calculation results of the average RMSE are in the final line, where the smallest value is produced by COLSE (Classical Ordinary Least Squares Exponential) fitting, which is 1.103 and the largest is RWLSE (Robust Weighted Least Squares Exponential) with an average value of 1.198 (TABLE 1).

TABLE 2 shows the variogram parameters obtained from the fitting results. Variogram parameters (nugget, sill, range) are used for Kriging estimation. The mathematical formula of practical exponential variogram showed in column two.

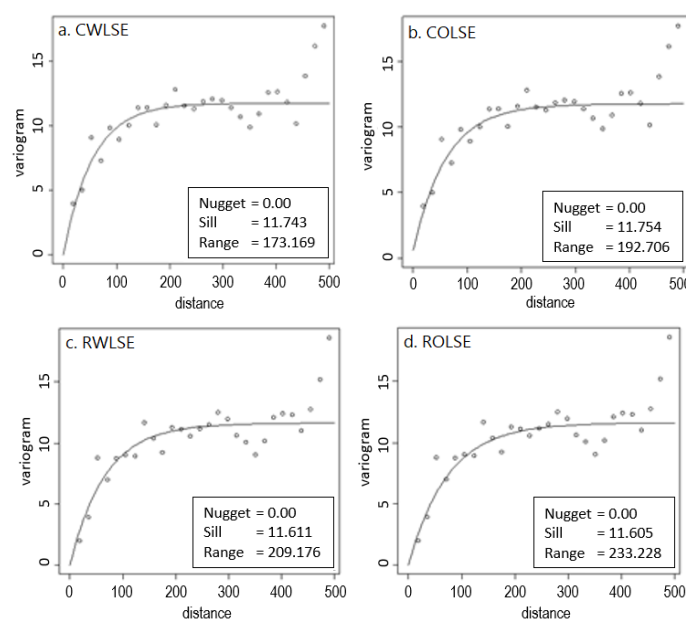


FIGURE 1. The graph of exponential semivariogram base

TABLE 3. Block kriging estimation includes average, variance and validation index for various fitting bases

Block	Mean-Kriging	Fitting based			
		CWLSE	COLSE	RWLSE	ROLSE
15×15	Prediction	4.611	4.586	4.568	4.548
	Variance	3.763	3.446	3.359	3.075
	Validation Index	0.190	0.249	0.265	0.324
25×25	Prediction	4.618	4.592	4.574	4.554
	Variance	3.774	3.482	3.396	3.110
	Validation Index	0.183	0.242	0.257	0.317
35×35	Prediction	4.590	4.564	4.546	4.525
	Variance	3.838	3.544	3.458	3.169
	Validation Index	0.164	0.233	0.239	0.300
50×50	Prediction	4.580	4.553	4.534	4.513
	Variance	3.955	3.653	3.565	3.268
	Validation Index	0.136	0.198	0.214	0.276
75×75	Prediction	4.673	4.645	4.627	4.605
	Variance	4.030	3.730	3.645	3.347
	Validation Index	0.138	0.197	0.212	0.273
100×100	Prediction	4.570	4.543	4.524	4.502
	Variance	4.233	3.919	3.820	3.520
	Validation Index	0.074	0.137	0.156	0.218

FIGURE 1 displayed empirical variogram visualization as equation (1) and (2) and fitting results as TABLE 2 (exponential). Because the RMSE value of the spherical model is greater than the exponential model, this paper does not show the fitting of the spherical variogram model. Overall, the results of fitting the variogram model in FIGURE 2 show that the nugget value is zero ($C_0=0$).

Mathematical equations of two variograms, namely spherical and exponential, results in fitting equation (as in TABLE 2). The sill is in the range of 11.605 (for robust fittings based on OLS exponential function) to 11.754 (for classical fittings OLS, based on exponential functions). Two areas of influence are generated by each robust fitting, RWLSE = 209.176 and ROLSE = 233.228. Fitting models based on classical variogram produce shorter spacing of influences, namely 173.169 (for CWLSE) and 192.706 (for COLSE).

TABLE 3 displays the variogram parameters obtained from the fitting results, where the first column is the category or basis used; the second and third columns, respectively, are a collection of sill and range values, namely variogram parameters which will later be used as the basis for Kriging predictions. From several blocks Kriging prediction produces an unpatterned value, but the predictive variance gets smaller as the block size gets smaller.

TOPSIS

The ranking score is based on validation index with 5 weighting scales. The assessment criteria (score) predictions are better if the index is getting bigger. The validation scoring results are shown in TABLE 4. As in columns 2 to 5, it is clear that the increase in the index of decision-matrix occurred in CWLSE, COLSE, RWLSE and ROLSE, respectively. This increase in value applies to each prediction block.

TABLE 4. Decision matrix states of the attributes and criteria for each block based on four fittings

Kriging Block size	Score value			
	CWLSE	COLSE	RWLSE	RWLSE
15×15	0.346	0.462	0.577	0.577
25×25	0.369	0.492	0.492	0.615
35×35	0.369	0.492	0.492	0.615
50×50	0.391	0.391	0.521	0.651
75×75	0.369	0.492	0.492	0.615
100×100	0.169	0.507	0.507	0.676

The normalized decision matrix values (successively for the four scores of each fitting result) as in TABLE 5 also increased proportionally to the values as in the attribute of decision matrix and as in the criteria of each block Kriging.

TABLE 5. Normalized decision matrix for each block based on four fitting models

Kriging block	Score			
	CWLSE	COLSE	RWLSE	RWLSE
15×15	1.477	1.963	2.454	2.454
25×25	1.477	1.969	1.969	2.462
35×35	1.477	1.969	1.969	2.462
50×50	1.465	1.465	1.953	2.441
75×75	1.477	1.969	1.969	2.462
100×100	0.465	1.395	1.395	1.859

Referring to TABLE 6 where the ideal-closeness occurs in 15×15 block Kriging, a distribution of predicted values can be shown.

Separation measure is a measurement of the distance from the alternative to a positive ideal solution and a negative ideal solution. Calculation of the ideal solution (positive and negative) is presented by TABLE 6. Column 2 is generated by formula (9). While column 3 is the result of calculations using formula (10). The relative proximity of the ideal solution is shown in columns 4 and 5 (TABLE 6).

TABLE 6. Separation value

i	S_i^+	S_i^-	C_i^+	C_i^-
1	1.0973	1.4722	0.573	0.427
2	1.2060	1.2060	0.500	0.500
3	1.2060	1.2060	0.500	0.500
4	1.6912	0.9764	0.366	0.634
5	1.2060	1.2060	0.500	0.500
6	1.5417	1.9166	0.554	0.446

FIGURE 2 illustrates the distribution of gold ore based on 15×15 block Kriging RWLSE base. The darker colour (black) indicates of high grade (in gram/ton Au) of ore distribution. Towards the higher of abscissa, the grade appears to be smaller. Even in any area it seems that the distribution of gold is no longer found.

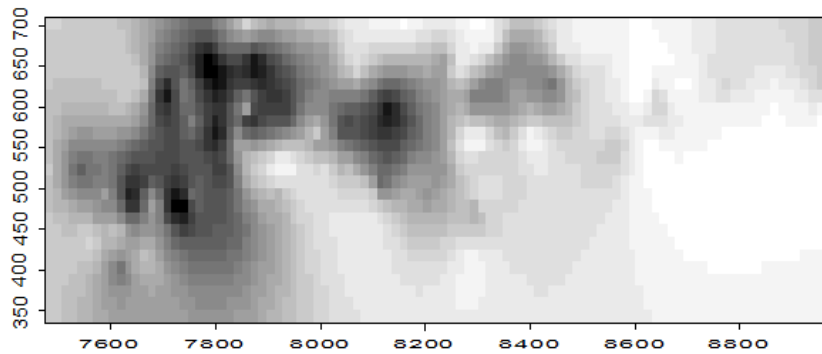


FIGURE 2. Distribution of gold predictive values based on 15×15 block Kriging of ROLSE model

CONCLUSION

Many conclusions of this research are,

1. Empirical variogram is a representation of spatial correlation between the samples. Therefore, the determination of lag distance becomes important as a fundamental construction of variogram models.
2. Variogram fittings produce parameters which are one of the determinants in Kriging estimation.
3. Block kriging estimation that refers to empirical variogram fitting with determination of regular lag distance (17.5 m), resulting in values where there is an increase in validation index starting from CWLSE, COLSE, RWLSE and ROLSE. An increase in the index value occurs in the estimation for each block size.
4. Based on ROLSE fitting, the most ideal proximity values of two criteria (positive and negative) occur in block kriging size of 15×15.

ACKNOWLEDGMENT

The author would like to thank the Institute for Research and Community Service UPN "Veteran "Yogyakarta Indonesia. Thank are also conveyed to PT. Aneka Tambang UBPE Pongkor who has provided the opportunity to obtain data in this research.

REFERENCES

- 1) Ilboudo H., Sawadogo S., Traoré A. S., Sama M., and Lompo M. 2018. Intrusion-Related Gold Mineralization: Inata Gold Deposit, Béléhourou District, Northern Burkina Faso (West-Africa). *Journal of African Earth Sciences*, 148: 52-58.
- 2) Stromberg J. M., Barr E., and Banerjee N. R. 2018. Early Carbonate Veining and Gold Mineralization in the Timmins Camp: Depositional Context of the Dome Mine Ankerite Veins. *Ore Geology Reviews*, 97: 55-73.
- 3) Murzin V. V., Chudnenko K. V., Palyanova G. A., Varlamov D. A., and Franco Pirajno F. 2018. *Physicochemical Model for The Genesis of Cu-Ag-Au-Hg Solid Solutions and Intermetallics in The Rodingites of the Zolotaya Gora Gold Deposit (Urals, Russia)*. *Ore Geology Reviews*, 93: 81-97.
- 4) Phillips G. N., and Powell R. 2015. Hydrothermal alteration in the Witwatersrand goldfields. *Ore Geology Reviews*, Vol. 65, Part 1: 245-273.
- 5) McCarroll R. J., Graham I. T., Fountain R., Privat K., and Woodhead J. 2014. The Ojolali Region, Sumatera, Indonesia: Epithermal Gold-Silver Mineralisation within the Sunda Arc. *Gondwana Research*, 26 (1): 218-240.
- 6) Morales M J., Silva R.C.F., Lobato L. M., Gomes S. D., and Banks D. A. 2016. *Metal Source and Fluid-Rock Interaction in the Archean BIF-hosted Lamego gold mineralization: Microthermometric and LA-ICP-MS analyses of fluid inclusions in quartz veins, Rio das Velhas greenstone belt, Brazil*. *Ore Geology Reviews*, 72 (1): 510-531.
- 7) Milési J.P., Marcoux E., Sitorus T., Simandjuntak M., J. Leroy J., and Baily L. 1999. Pongkor (West Java): A Pliocene Supergene-Enriched Epithermal Au-Ag-(Mn) Deposit. *Journal of Mineral Deposita* 34: 131-149.
- 8) Wambo J.D.T., Ganno S., Lahe Y.S.D., Nono G.J.K., and Nzenti J. P. 2018. Geostatistical and GIS Analysis of the Spatial Variability of Alluvial Gold Content in Ngoura-Colomines Area, Eastern Cameroon: Implications for The Exploration of Primary Gold Deposit. *Journal of African Earth Sciences*, 142: 138-157.
- 9) Qingsong Du, Guoyu Li, Yu Zhou, Gang Wu1, Mingtang, Chai, Fayong Li. 2021. Distribution Characterization Study of the Heavy Metals for a Mining Area of East Tianshan Mountain in Xinjiang Based on the Kriging Interpolation Method. *The 7th International Conference on Environmental Science and Civil Engineering*. IOP Conf. Series: Earth and Environmental Science 719: 042063.
- 10) Jiachang Qian, Jiaxiang Yi, Yuansheng Cheng, Jun Liu, Qi Zhou. 2020. A Sequential Constraints Updating Approach for Kriging Surrogate Model-assisted Engineering Optimization Design Problem. *Journal of Engineering with Computers*, 36: 993-1009.

- 11) Cressie N.A.C. 1993. *Statistics for Spatial Data*. New York. Chichester. Toronto. Brisbane. Singapore: John Wiley & Sons Inc.
- 12) Nezhad Y. A., Moradzadeh A., and Kamali M. R. 2018. A New Approach to Evaluate Organic Geochemistry Parameters by Geostatistical Methods: A Case Study from Western Australia. *Journal of Petroleum Science and Engineering*, 169: 813-824.
- 13) Ribeiro M. C., Pinho P., Branquinho C., Llop E., and Pereira M. J. 2016. Geostatistical Uncertainty of Assessing Air Quality Using High-Spatial-Resolution Lichen Data: A Health Study in The Urban Area of Sines, Portugal. *Science of The Total Environment*, 562: 740-750.
- 14) Fabbri, P., Gaetan, C., Sartore, L. and Libera, N.D. 2020. Subsoil Reconstruction in Geostatistics beyond Kriging: A Case Study in Veneto (NE Italy). *Journal of Hydrology*, 7: 1 - 15.
- 15) Pajač M., Halecki W., and Gašiorek M. 2017. Accumulative Response of Scots Pine (*Pinus sylvestris* L.) and Silver Birch (*Betula pendula* Roth) to Heavy Metals Enhanced by Pb-Zn Ore Mining and Processing Plants: Explicitly Spatial Considerations of Ordinary Kriging Based on a GIS Approach. *Journal of Chemosphere*, 168: 851-859.
- 16) Zulkarnain I., and Bargawa W. S. 2018. Classification of Coal Resources Using Drill Hole Spacing Analysis (DHSA). *Journal of Geological Resource and Engineering*, 6: 151-159.
- 17) Akbar D. A. 2012. Reserve Estimation of Central Part of Choghart North Anomaly Iron Ore Deposit Through Ordinary Kriging Method. *International Journal of Mining Science and Technology*, 22 (4): 573-577.
- 18) Pue, J.D., Yves-Dady Botula, Y-D., Nguyen, P.M., Meirvenne, M.V., Cornelis, W.M. 2021. Introducing a Kriging-based Gaussian Process approach in pedotransfer functions: Evaluation for the prediction of soil water retention with temperate and tropical datasets. *Journal of Hydrology*, 597: 125770.
- 19) Ren J., Chen J., Han L., Wang M., and Li F. 2018. Spatial Distribution of Heavy Metals, Salinity and Alkalinity in Soils Around Bauxite Residue Disposal Area. *Science of the Total Environment*, 628-629: 1200-1208.
- 20) Amri, N.A., Jemain, A. A. and Wan Fuad, W.H. 2014. Ordinary kriging based on OLS-WLS fitting semivariogram: Case of gold vein precipitation, *Proceedings of the 3rd International Conference on Mathematical Sciences*. AIP Conf. Proc. 1602: 1039-1045.
- 21) Li Z., Zhang X., Clarke K. C., Liu G., and Zhu R. 2018. An Automatic Variogram Modeling Method with High Reliability Fitness and Estimates. *Journal of Computers & Geosciences*, 120: 48-59.
- 22) Sun Y., Chang X., and Guan Y. 2018. Flexible and Efficient Estimating Equations for Variogram Estimation, *Computational Statistics & Data Analysis*, 122: 45-58.
- 23) Hanke J. R., Fischer M. P., and Pollyea R. M. 2018. Directional Semivariogram Analysis to Identify and Rank Controls on the Spatial Variability of Fracture Networks. *Journal of Structural Geology*, 108: 34-51.
- 24) Matheron G. 1963. *Principles of Geostatistics*. *Journal of Economic Geology*, 58: 1246-1266.

- 25) DiCiccio C. J., Romano J. P., and Wolf M. 2018. Improving Weighted Least Squares Inference. *Econometrics and Statistics*, In press, corrected proof, Available online 20 June 2018.
- 26) Romano J. P., and Wolf M. 2017. Resurrecting Weighted Least Squares. *Journal of Econometrics*, 197, (1): 1-19.
- 27) Chakraborty S., Man T., Paulette L., Deb S., and Frazier M. 2017. Rapid assessment of smelter/mining soil contamination via portable X-ray fluorescence spectrometry and indicator kriging. *Journal of Geoderma*, 306: 108-119.
- 28) Dehaine Q., Filippov L. O., and Royer J. J. 2016. Comparing Univariate and Multivariate Approaches for Process Variograms: A Case Study. *J. Chemometrics and Intelligent Laboratory Systems*, 152: 107-117.
- 29) El-Shirbeny M., and Abdellatif A. B. 2017. Reference Evapotranspiration Borders Maps of Egypt Based on Kriging Spatial Statistics Method. *International Journal of GEOMATE*, 37 (13): 1-8.
- 30) Inazumi S., Urakami K., Ohtsuka S., Saeki O., and Shishido K. 2016. Prediction of Spatial Distribution on Soil Surveying Values Using Geostatistics Methods. *International Journal of GEOMATE*, 20 (10): 1828-1833.
- 31) Ahmadi M. R., and Shahabi R. S. 2018. Cutoff grade Optimization in open Pit Mines Using Genetic Algorithm. *J. Resources Policy*, 55: 184-191.
- 32) Kleijnen J.P.C., and Mehdad E. 2016. *Estimating the Variance of the Predictor in Stochastic Kriging, Simulation Modelling Practice and Theory*. 66: 166-173.
- 33) Liu H., Cai J., and Ong Y. S. 2017. An Adaptive Sampling Approach for Kriging Metamodeling by Maximizing Expected Prediction Error. *Journal of Computers & Chemical Engineering*. 106: 171-182.
- 34) Ribeiro P.J.Jr., and Diggle P.J. 2001. *geoR: A Package for Geostatistical Analysis*. R-News, 2 (1): 15-18.
- 35) Zareie A., Sheikahmadi A., and Khamforoosh K. 2018. *Influence Maximization in Social Networks Based on TOPSIS, Expert Systems with Applications*, 108: 15 October 2018: 96-107.
- 36) Lee H. C., Chang C. T. 2018. Comparative Analysis of MCDM Methods for Ranking Renewable Energy Sources in Taiwan. *Journal of Renewable and Sustainable Energy Reviews*, 92: 883-896.
- 37) Yager R. R. 2018. Categorization in Multi-Criteria Decision Making, *Information Sciences*, 460-461: 416-423.
- 38) Asadabadi M. R. 2018. *The Stratified Multi-Criteria Decision-Making Method. Knowledge-Based Systems, In press, corrected proof*, Available online 6 July 2018.
- 39) Hassan A., and Issa U. H. 2014. Developing a Decision-Making Model for Reinforced Concrete Columns Strengthening. *International Journal of GEOMATE*, 17 (9): 1333-1341.
- 40) Yoon K. P., Kim W. K. 2017. The behavioral TOPSIS. *Expert Systems with Applications*, 89: 266-272.
- 41) Nowak M. 2017. Defining Project Approach Using Decision Tree and Quasi-Hierarchical Multiple Criteria Method. *Procedia Engineering*, 172: 791-799.